Poly(Alumosiloxanes) as Matrixes for the Immobilization of Catalytically Active Ruthenium(II) Complexes[1]

Ekkehard Lindner,*,† Andreas Jäger,† Friedrich Auer,† Peter Wegner,† Hermann A. Mayer,*,†,§ Andreas Benez,‡ Dorothea Adam,‡ and Erich Plies‡

Institut für Anorganische Chemie der Universität Tübingen, Auf der Morgenstelle 18, D-72076 Tübingen, Germany, and Institut für Angewandte Physik der Universität Tübingen, Auf der Morgenstelle 10, D-72076 Tübingen, Germany

Received May 8, 1997. Revised Manuscript Received November 10, 1997

The trimethoxysilyl-(T)-functionalized ruthenium(II) complexes *cis*-Cl(H)Ru(CO)(P∼O)$_3$ [**2a(T^0)$_3$**, **2b(T^0)$_3$**, and **2c(T^0)$_3$**] (T = T-type silicon atom, three oxygen neighbors, P∼O = P-coordinated ether-phosphines with different spacer lengths) were sol−gel processed with different silicon-containing precursors {tetraethoxysilane [Si(OEt)$_4$, **Q^0**, Q = Q-type silicon atom, four oxygen neighbors], methyltrimethoxysilane [MeSi(OMe)$_3$, **T^0**, T = T-type silicon atom, three oxygen neighbors], or dimethyldiethoxysilane [Me$_2$Si(OEt)$_2$, **D^0**, D = D-type silicon atom, two oxygen neighbors]} and aluminum 2-propanolate [Al(O*i*Pr)$_3$]. All components are simultaneously polycondensed to result in the poly(alumosiloxane)-bound ruthenium complexes [**2(a,b,c)(T^n)$_3$(Q^k,T^m,D^i)$_y$(Al)$_z$**] [**(Al)** denotes (Al$_2$O$_3$)$_{1/2}$]. From ^{31}P and ^{13}C CP/MAS NMR as well as IR spectroscopy it can be concluded that the complex fragment *cis*-Cl(H)Ru(CO)(P∼O)$_3$ is preserved during the immobilization. The aluminum is incorporated as tetrahedrally coordinated AlO$_4$ units while 6-fold-coordinated AlO$_6$ groups are built in as interstitials. Stoichiometric formulas and structural models of the carrier matrixes are derived from ^{27}Al and ^{29}Si solid-state NMR spectroscopy, including ^{27}Al{^{1}H} REDOR and ^{1}H−^{27}Al CP/MAS NMR techniques, as well as energy-dispersive X-ray spectroscopy (EDX). The dynamic behavior of the various catalysts is investigated by 2D WISE spectroscopy and ^{31}P CP/MAS NMR line widths. The immobilized complexes act as hydrogenation catalysts of *n*-butenal and are easy to separate from the reaction mixture by simple centrifugation.

Introduction

Chemical systems in which the reactive centers are bound to polymeric matrixes are a research field of ongoing interest.[2−4] The immobilization of transition metal complexes leads to systems that are able to combine the advantages of homogeneous and heterogeneous catalysis. In particular the presence of an adequate solvent or substrate (mobile phase) gives rise to a swelling of the polymers (stationary phase). The resulting mixture of a mobile and a stationary phase on a molecular scale is called an "interphase". Interphases are able to combine the adjustable activities and selectivities of homogeneous reaction types with a repeated use of the catalyst.[1,5−7]

Various strategies to build up stationary phases, consisting of the matrix, the spacer, and the reactive center, have been developed. Surface-modified silica gel is widely used as a carrier matrix, since it is chemically resistant and its surface properties are well-defined.[8−10] However, there are some problems with these systems: (i) the loading of the catalysts is low and limited by the external surface of the silica gel; (ii) the catalysts leach from the support during catalysis due to low degrees of condensation of the ligands to the silica gel surface; (iii) poor swelling abilities of the silica gel reduce the formation of interphases.

One approach to overcome these problems is the simultaneous co-condensation of organo-(T)-silyl-functionalized transition metal complexes with D, D−C$_n$−D, T, or Q alkoxysilanes [D = R$_2$Si(OR′)$_2$, D−C$_n$−D = MeSi(OR′)$_2$(CH$_2$)$_n$(R′O)$_2$SiMe, T = RSi(OR′)$_3$, Q = Si(OR′)$_4$; R, R′ = Me, Et] (sol−gel process; D-, T-, and Q-type silicon with two, three, and four oxygen neighbors, respectively).[6,11−13] The obtained two- and three-dimensional networks are stationary phases, in which

* To whom correspondence should be sent.
† Institut für Anorganische Chemie.
§ E-mail: hermann.mayer@uni-tuebingen.de.
‡ Institut für Angewandte Physik.

(1) Supported Organometallic Complexes Part 15. Part 14: Lindner, E.; Schneller, T.; Auer, F.; Wegner, P.; Mayer, H. A. *Chem. Eur. J.* **1997**, *3*, 1833.
(2) Hartley, F. R. *Supported Metal Complexes*; D. Reidel Publishing Co.: Boston, 1985.
(3) Iwasawa, Y. I. *Tailored Metal Complexes*, D. Reidel Publishing Co.: Boston, 1986.
(4) Deschler, U.; Kleinschmit, P.; Panster, P. *Angew. Chem., Int. Ed. Engl.* **1986**, *25*, 236.
(5) Lindner, E.; Kemmler, M.; Schneller, T.; Mayer, H. A. *Inorg. Chem.* **1995**, *34*, 5489.
(6) Lindner, E.; Kemmler, M.; Mayer, H. A.; Wegner, P. *J. Am. Chem. Soc.* **1994**, *116*, 348.
(7) Lindner, E.; Jäger, A.; Auer, F.; Wielandt, W.; Wegner, P. *J. Mol. Catal.*, in press.
(8) Sindorf, W. W.; Maciel, G. E. *J. Am. Chem. Soc.* **1983**, *105*, 3767.
(9) Bayer, E.; Albert, K.; Reiners, J.; Nieder, M.; Müller, D. *J. Chromatogr.* **1983**, *264*, 197.
(10) Blümel, J. *Inorg. Chem.* **1994**, *33*, 5050.
(11) Lindner, E.; Jäger, A.; Schneller, T.; Mayer, H. A. *Chem. Mater.* **1997**, *9*, 81.

S0897-4756(97)00342-6 CCC: $15.00
Published on Web 01/01/1998

the amount of the catalyst, the polarity of the matrix, and the mobility of the reactive centers can be varied in a wide range. Furthermore the detachment of the reactive centers is strongly reduced by the high degrees of condensation of these materials.

Another parameter that has been varied systematically in the case of polysiloxane-bound ruthenium complexes is the length of the spacer that connects the reactive center covalently to the supporting matrix.[11] It has been shown that an extension of the alkyl chains from *n*-propyl (C3) via *n*-hexyl (C6) to *n*-octyl (C8) enhances the mobility of the reactive centers and leads to higher conversions and selectivities in the hydrogenation of *n*-butenal.[7]

Recently it was demonstrated that the introduction of ionic charges improves the separability of the stationary phase from the reaction mixture.[14] The ionic charges can be introduced into the matrix by either network modifiers (e.g. Na^+, Mg^{2+}) or network builders (e.g. B, Al, P). Network-modified polysiloxanes, for example, Mg^{2+}-doped polysiloxanes, have been applied successfully in catalysis.[6] However, the incorporation of Mg^{2+} lowers the degree of cross-linkage, which may cause leaching of the reactive centers from the matrix. Thus networks in which the ionic charges are introduced via network builders, for example, poly(alumosiloxanes), have to be preferred, since aluminum is incorporated into the matrix via covalent bonds and accounts for ionic charges.

The aim of the present study is to investigate if the variable properties of polysiloxane matrixes can be transferred to poly(alumosiloxane) matrixes. We therefore prepared poly(alumosiloxane)-bound ruthenium complexes containing different silicon sol−gel precursors, for example, **Q⁰**, **T⁰**, **D⁰**, and different lengths of spacer (*n*-propyl, *n*-hexyl, and *n*-octyl).

The new materials were characterized by multinuclear solid-state NMR spectroscopy.[15−17] The stereochemistry of the metal complexes, the integrity of the spacers, and the ligand backbone were established by ^{31}P and ^{13}C CP/MAS NMR spectroscopy. ^{29}Si CP/MAS and ^{27}Al MAS NMR spectroscopy were applied to characterize the poly(alumosiloxane) support. $^{27}Al\{^1H\}$ rotational-echo double-resonance (REDOR) and $^1H-^{27}Al$ CP/MAS NMR techniques have been employed to investigate the structure of the aluminum species more precisely. Information about the mobilities of the compounds are derived from $^1H-^{13}C$ wide-line separation (WISE) NMR spectroscopy and from ^{31}P CP MAS NMR line widths. Furthermore energy-dispersive X-ray spectroscopy (EDX) and scanning electron microscopy (SEM) were used to describe the materials. Prelimary catalytic results were presented in the case of the hydrogenation of *n*-butenal.

Scheme 1. Schematic Representation of the Sol−Gel Process[a]

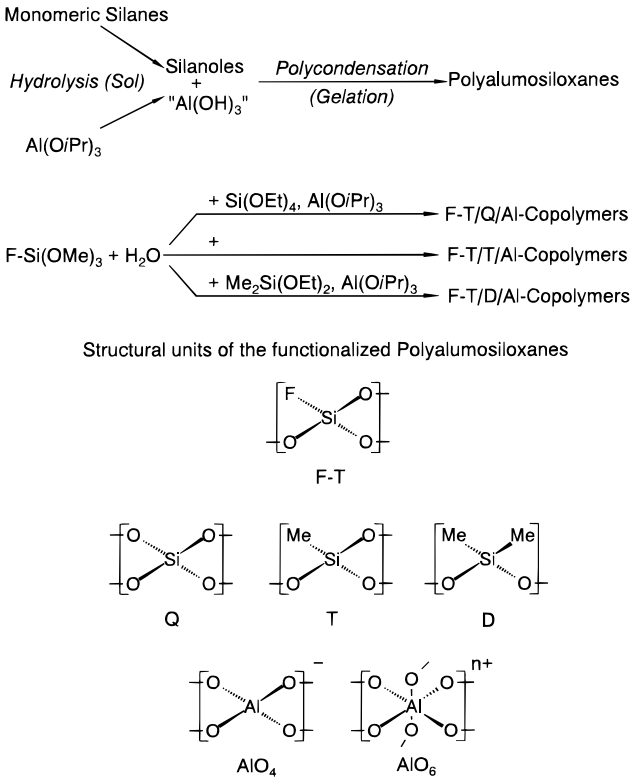

[a] F = [*cis*-Cl(H)Ru(CO)]$_{1/3}$P(Ph)(CH$_2$CH$_2$OMe)(CH$_2$)$_x$−, x = length of the spacer [x = 3 (**a**), 6 (**b**), 8(**c**)]. Q: Q type silicon atom (four oxygen neighbors). T: T type silicon atom (three oxygen neighbors). D: D type silicon atom (two oxygen neighbors). AlO_6^{n+} = positively charged AlO_6 units; n depends on the coordination sphere of the aluminum (H_2O, OH, or SiO).

Results and Discussion

Monomeric Complexes [2(a,b,c)(T⁰)$_3$].[18] The monomeric complexes *cis*-Cl(H)Ru(CO)(P∼O)$_3$ [**2a(T⁰)$_3$**, **2b-(T⁰)$_3$**, **2c(T⁰)$_3$**; see Scheme 2] were prepared by substitution of triphenylphosphine in *cis*-Cl(H)Ru(CO)(PPh$_3$)$_3$ for the more basic ether-phosphines [**1(a,b,c)(T⁰)**; see ref 11 and Experimental Section]. The corresponding ether-phosphine ligands **1(a,b,c)(T⁰)** with *n*-propyl, *n*-hexyl, and *n*-octyl spacers, respectively (see Scheme 2), can be prepared in a few steps and with good yields by procedures given in the literature.[11,19] These "hemilabile" ligands are able to coordinate strongly to the metal center via the phosphorus atom, while the weaker donor in the form of an ether moiety is able to take over the function of an intramolecular solvent in a catalytic cycle.[21]

Sol−Gel Processing. The aluminum-containing F−T/Q/Al, F−T/T/Al, and F−T/D/Al copolymers of **2-(a,b,c)(T₀)$_3$** [18] {F = [*cis*-Cl(H)Ru(CO)]$_{1/3}$P(Ph)(CH$_2$CH$_2$-

(12) Lindner, E.; Schneller, T.; Mayer, H. A.; Bertagnolli, H.; Ertel, T. S.; Hörner, W. *Chem. Mater.* **1997**, *9*, 1524.
(13) Brinker, C. J.; Scherer, G. W. *Sol Gel Science*; Academic Press: London, 1990.
(14) Lindner, E.; Jäger, A.; Kemmler, M.; Auer, F.; Wegner, P.; Mayer, H. A.; Benez, A.; Plies, E. *Inorg. Chem.* **1997**, *36*, 862.
(15) Fyfe, C. A. *Solid State NMR for Chemists*; CRC Press: Guelph, ON, 1984.
(16) Engelhardt, G.; Michel, D. *High-Resolution Solid-State NMR of Silicates and Zeolites*; John Wiley and Sons: Chichester, New York, 1987.
(17) Schmidt-Rohr, K.; Spiess, H. W. *Multidimensional Solid State NMR and Polymers*; Academic Press: London, 1994.
(18) Nomenclature of the compounds. *Integer*: type of reactive center (**1** = ligand, **2** = complex). *Small letter*: type of spacer (**a** = *n*-propyl, **b** = *n*-hexyl, **c** = *n*-octyl). *Capital letter*: type of silicon species (**Q** = four oxygen bonds, **T** = three oxygen bonds, **D** = two oxygen bonds). *Subscribt*: stoichiometry of the silicon species. *Superscript*: number of Si−O−Si bonds. (**Al**) = (Al$_2$O$_3$)$_{1/2}$.
(19) Lindner, E.; Bader, A.; Glaser, E.; Pfleiderer, B.; Schumann, W.; Bayer, E. *J. Organomet. Chem.* **1988**, *355*, 45.
(20) Bader, A.; Lindner, E. *Coord. Chem. Rev.* **1991**, *108*, 27.
(21) Fuchs, E.; Oppolzer, H.; Rehme, H. *Particle Beam Microanalysis*; VCH: Weinheim, 1990.

Scheme 2. Synthetic Route to the Monomeric Ruthenium Complexes 2A(T^0)$_3$, 2B(T^0)$_3$, 2C(T^0)$_3$[a]

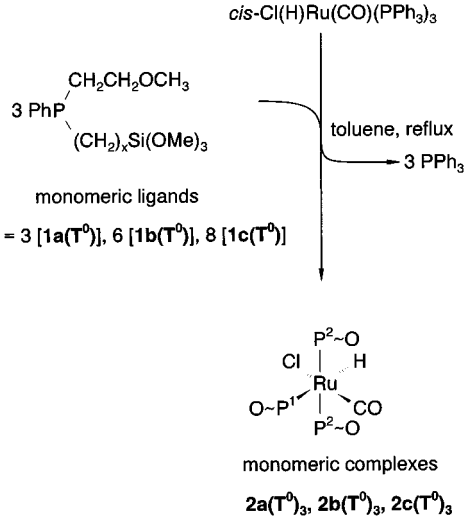

[a] P∼O: η^1-coordinated ether phosphine ligand **1a(T^0)**, **1b(T^0)**, **1c(T^0)**.

Scheme 3. Schematic Presentation of the Polycondensation[a]

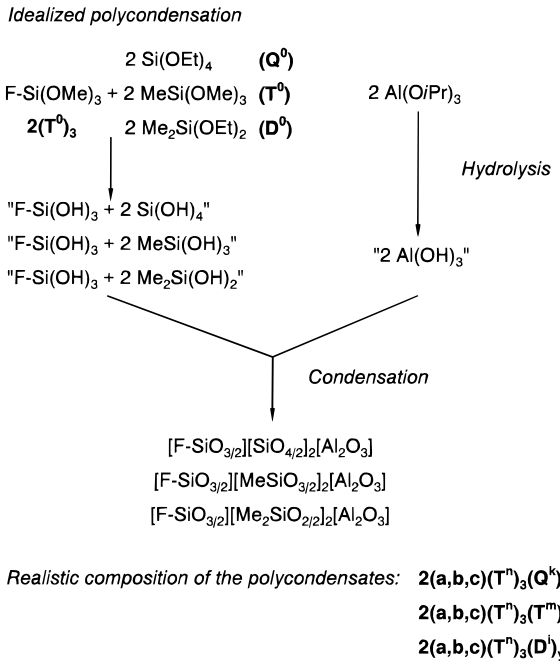

Realistic composition of the polycondensates: **2(a,b,c)(T^n)$_3$(Q^k)$_y$(Al)$_z$**
2(a,b,c)(T^n)$_3$(T^m)$_y$(Al)$_z$
2(a,b,c)(T^n)$_3$(D^i)$_y$(Al)$_z$

[a] F = [*cis*-Cl(H)Ru(CO)]$_{1/3}$P(Ph)(CH$_2$CH$_2$OMe)(CH$_2$)$_x$−. Q: Q type silicon atom (four oxygen neighbors). T: T type silicon atom (three oxygen neighbors). D: D type silicon atom (two oxygen neighbors). *k*, *i*, *m*, *n* = number of Si−O−Si bonds. (Al): formal description of (Al$_2$O$_3$)$_{1/2}$; *y* = real number of co-condensed Q, T, D silicon atoms. *z* = real number of co-condensed (Al) units.

OMe)(CH$_2$)$_x$−} were obtained in a simultaneous sol−gel process (see Scheme 3). In the first step specified amounts of Al(O*i*Pr)$_3$ acting as an aluminum-containing precursor were suspended in MeOH and hydrolyzed with an excess of water. Subsequently the resulting sols were added to mixtures of the corresponding monomeric complexes *cis*-Cl(H)Ru(CO)(P∼O)$_3$ [**2(a,b,c)(T^0)$_3$**] (Scheme 2) and the co-condensation agents Si(OEt)$_4$ (**Q^0**), MeSi(OMe)$_3$ (**T^0**), or Me$_2$Si(OEt)$_2$ (**D^0**).[14] To start the hydrolysis Sn(OAc)$_2$(*n*-Bu)$_2$ is necessary as a catalyst. The polycondensations are initiated with 1 M NaOH. In the course of the addition of aqueous NH$_4$HCO$_3$ voluminous gels precipitated. After washing and drying, the gels were obtained as ultrafine powders. The tiny, rounded particles of the gel **2a(T^n)$_3$(Q^k)$_4$(Al)$_4$** (*n* = 0−3, *k* = 0−4; number of Si−O−Si bonds) are displayed in Figure 1. The particle sizes of the material are in the range of 5 μm. The labeling of all polycondensation products is summarized in Table 1.

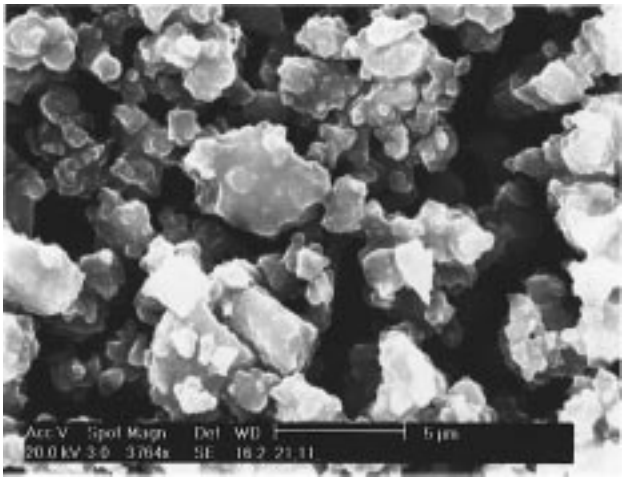

Figure 1. Scanning electron micrograph of **2a(T^n)$_3$(Q^k)$_4$(Al)$_4$**.

Characterization of the Poly(alumosiloxane) Matrixes by Energy-Dispersive X-ray Spectroscopy (EDX) and ^{29}Si, ^{27}Al Solid-State NMR Spectroscopy. The elemental composition of the obtained gels was determined by energy-dispersive X-ray spectroscopy (EDX) (see Table 2).[21] The experimentally determined Ru/P ratio of 1:3 for all materials shows that the ruthenium complex fragment *cis*-Cl(H)Ru(CO)(P∼O)$_3$ exists in the matrix. It can be concluded that neither ruthenium nor uncomplexed ligand has been washed out during the sol−gel procedure. This result is confirmed by ^{31}P CP/MAS NMR and IR spectroscopic investigations (see below). From an ideal sol−gel process it is expected that the ratios of Ru/P/Si/Al are equal to 1:3:9:6 for all samples. However, great discrepancies between the applied stoichiometries and the real compositions are found in most materials. Only **2c(T^n)$_3$(Q^k)$_6$(Al)$_6$** reveals the complete amount of the co-condensation agents **Q^0** [Si(OEt)$_4$] and Al(O*i*Pr)$_3$. In the other F−T/Q/Al copolymers approximately 15 and 30% of the **Q^k** groups are missing, which is more than the estimated limits of error of ±10% for the EDX method (see Experimental Section). In the case of the F−T/T/Al co-condensates one-half of the employed **T^m** (*m* = 0−3; number of Si−O−Si bonds) groups are washed out, and in the case of the F−T/D/Al copolymers only one of six moles of **D^i** (*i* = 0−2; number of Si−O−Si bonds) groups were found in the matrixes (Table 2). The real aluminum contents vary between 40 and 100% of the employed stoichiometries. Thus considerable amounts of the co-condensation agents were washed out as silicic acid derivatives or soluble oligomers during the sol−gel process. This result is in agreement with earlier investigations in which it was found that depending on the type of the sol−gel process employed specific amounts of co-condensation agents were washed out during the heterogenization.[6,11] However, realistic formulas of the

Table 1. Labeling of the Copolymers[18]

monomeric complexes	spacer length[a]	silicon-containing co-condensate		
		$\mathbf{Q^0}$ [$Si(OEt)_4$]	$\mathbf{T^0}$ [$MeSi(OMe)_3$]	$\mathbf{D^0}$ [$Me_2Si(OEt)_2$]
$\mathbf{2a(T^0)_3}$	3	$\mathbf{2a(T^n)_3(Q^k)_4(Al)_4}$	$\mathbf{2a(T^n)_3(T^m)_{2.7}(Al)_{4.2}}$	$\mathbf{2a(T^n)_3(D^i)_1(Al)_{2.5}}$
$\mathbf{2b(T^0)_3}$	6	$\mathbf{2b(T^n)_5(Q^k)_6(Al)_{4.3}}$	$\mathbf{2b(T^n)_3(T^m)_3(Al)_{4.5}}$	$\mathbf{2b(T^n)_3(D^i)_{0.8}(Al)_{2.8}}$
$\mathbf{2c(T^0)_3}$	8	$\mathbf{2c(T^n)_3(Q^k)_6(Al)_6}$	$\mathbf{2c(T^n)_3(T^m)_{3.5}(Al)_5}$	$\mathbf{2c(T^n)_3(D^i)_{0.8}(Al)_{5.3}}$

[a] Number of methylene groups between phosphorus and silicon in ligand **1**.

Table 2. Composition of the Materials According to EDX Spectroscopy[a]

material	elements[b]							
	Ru		P		Si		Al	
	ideal	real	ideal	real	ideal	real	ideal	real
$\mathbf{2a(T^n)_3(Q^k)_4(Al)_4}$	1.0	1.0	3.0	3.0	9.0	7.0	6.0	4.0
$\mathbf{2b(T^n)_3(Q^k)_5(Al)_{4.3}}$	1.0	1.0	3.0	3.0	9.0	8.0	6.0	4.3
$\mathbf{2c(T^n)_3(Q^k)_6(Al)_6}$	1.0	1.0	3.0	3.0	9.0	9.0	6.0	6.0
$\mathbf{2a(T^n)_3(T^m)_{2.7}(Al)_{4.2}}$	1.0	1.0	3.0	3.0	9.0	5.7	6.0	4.2
$\mathbf{2b(T^n)_3(T^m)_3(Al)_{4.5}}$	1.0	1.0	3.0	3.0	9.0	6.0	6.0	4.5
$\mathbf{2c(T^n)_3(T^m)_{3.5}(Al)_5}$	1.0	1.0	3.0	3.0	9.0	6.5	6.0	5.0
$\mathbf{2a(T^n)_3(D^i)_1(Al)_{2.5}}$	1.0	1.0	3.0	3.0	9.0	4.0	6.0	2.5
$\mathbf{2b(T^n)_3(D^i)_{0.8}(Al)_{2.8}}$	1.0	1.0	3.0	3.0	9.0	3.8	6.0	2.8
$\mathbf{2c(T^n)_3(D^i)_{0.8}(Al)_{5.3}}$	1.0	1.0	3.0	3.0	9.0	3.8	6.0	5.3

[a] Additionally C, O, Cl, and minor amounts of Sn were found in the EDX spectrum. [b] The numbers of individual elements represent the amount of atoms per monomeric unit. The values of P were set equal to 3.

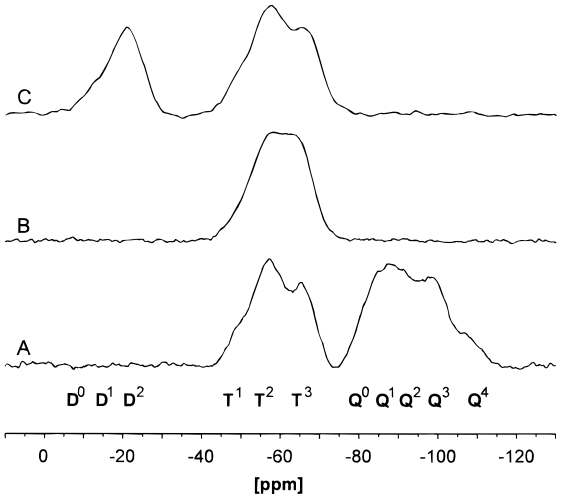

Figure 2. ^{29}Si CP/MAS NMR spectra of the materials $\mathbf{2a(T^n)_3(Q^k)_4(Al)_4}$ (A), $\mathbf{2a(T^n)_3(T^m)_{2.7}(Al)_{4.2}}$ (B), and $\mathbf{2a(T^n)_3(D^i)_1(Al)_{2.5}}$ (C) including the chemical shift ranges of the different silyl species.

copolymers can be derived by the EDX results and are in reasonable agreement with the elemental analysis (see Experimetal Section).

In Figure 2 the ^{29}Si CP/MAS NMR spectra of the polymers $\mathbf{2a(T^n)_3(Q^k)_4(Al)_4}$, $\mathbf{2a(T^n)_3(T^m)_{2.7}(Al)_{4.2}}$, and $\mathbf{2a(T^n)_3(D^i)_1(Al)_{2.5}}$ are displayed. They reveal the typical resonances of the different silyl groups, in particular the $\mathbf{D^i}$ moieties from −9 to −23 ppm, the $\mathbf{T^{n,m}}$ species from −48 to −66 ppm, and the $\mathbf{Q^k}$ groups from −82 to −110 ppm.[22,23] The lower resolutions of the spectra compared to the ^{29}Si CP/MAS NMR spectra of pure polysiloxane matrixes indicate the incorporation of aluminum into the matrix. Both, Si−OH and Si−O−Al groups lead to a downfield shift of the ^{29}Si resonance compared to the fully cross-linked Si−O−Si moiety.[16,24]

Deconvolution of the spectra yields mainly three $\mathbf{D^i}$ (i = 0−2), three $\mathbf{T^{n,m}}$ (n, m = 1−3), and five $\mathbf{Q^k}$ subspecies (k = 0−4) (see Table 3 and Experimental Section). Taking the cross-polarization dynamics into account, the corrected amounts of I_0 of each individual silyl species can be calculated (see Table 3). The obtained T/D ratios of the F−T/D/Al copolymers agree with the EDX results and confirm that only one-sixth of the employed $\mathbf{D^0}$ groups are found in these materials (Table 2). In case of the F−T/Q/Al copolymers the amounts of $\mathbf{Q^k}$ groups determined by ^{29}Si CP/MAS NMR spectroscopy are lower than expected from the EDX investigations. This can be explained in terms of "bulk" $\mathbf{Q^4}$ groups which do not have any protons within the range of four bonds and are thus not detectable by cross-polarization.[6] Integration of the ^{29}Si MAS (SPE) NMR spectra of these three compounds verifies this suggestion. However, these spectra exhibit only poor signal-to-noise ratios within reasonable measuring times.

In the ^{27}Al MAS NMR spectra of the compounds two resonances are observed at δ = 55 and 2 (see Figure 3). The resonance shifts are typical for tetrahedrally and octahedrally coordinated AlO_4 and AlO_6 units, respectively.[16,24] The amount of AlO_4 versus AlO_6 units is decreasing on going from F−T/Q/Al via F−T/T/Al to F−T/D/Al copolymers. The tetrahedrally coordinated AlO_4 species are incorporated into the polysiloxane framework and can act formally as negatively charged SiO_4 sites. The increasing amount of AlO_6 groups in F−T/T/Al and F−T/D/Al is thus correlated with the formation of aluminum-rich domains consisting of pure alumoxane.

^{27}Al{^{1}H} REDOR and ^{1}H−^{27}Al CP/MAS NMR Spectroscopic Investigations. To get a more detailed insight into how the two aluminum species are present in the matrixes ^{27}Al{^{1}H} rotational-echo double-resonance (REDOR) NMR and ^{1}H−^{27}Al CP/MAS NMR techniques have been employed.[25−27]

(22) Maciel, G. E.; Sindorf, D. W. *J. Am. Chem. Soc.* **1980**, *102*, 7606.
(23) Williams, E. A. NMR Spectroscopy of Organosilicon Compounds. In *Chemistry of Organic Silicon Compounds*; Patai, S., Rappoport, Z., Eds.; Wiley: New York, 1989.
(24) Eckert, H. *Prog. Nucl. Magn. Reson. Spectrosc.* **1992**, *24*, 159.
(25) Gullion, T.; Schaefer, J. *J. Magn. Reson.* **1989**, *81*, 196.

Table 3. Relative I_0,[a] T_{SiH},[b] and $T_{1\rho H}$[c] Data of the Silyl Groups of the Co-condensates

compound	relative I_0 data of the silyl species								ratio	T_{SiH} [ms]						$T_{1\rho H}$ [ms]
F−T/Q/Al	T^1	T^2	T^3	Q^0	Q^1	Q^2	Q^3	Q^4	T/Q	T^2	T^3	Q^1	Q^2	Q^3	Q^4	
2a(T^n)$_3$(Q^k)$_4$(Al)$_4$	1.1	5.4	3.5	0.2	4.9	0.7	5.6	1.2	3:3.8	0.87	1.27	0.85		0.99	1.82	4.7
2b(T^n)$_3$(Q^k)$_5$(Al)$_{4.3}$	0.4	4.2	5.4	1.1	2.1	2.4	7.6	1.3	3:4.4	1.21	1.48	1.03	1.36	1.61	3.12	4.6
2c(T^n)$_3$(Q^k)$_6$(Al)$_6$	2.2	4.5	3.3	0.9	4.8	2.7	5.4	1.5	3:4.6	1.11	1.46	0.90	0.90	0.82	1.60	4.0
F−T/T/Al	T^1	T^2	T^3							T^2	T^3					
2a(T^n)$_3$(T^m)$_{2.7}$(Al)$_{4.2}$	0.8	4.2	5.1							1.23	1.44					7.2
2b(T^n)$_3$(T^m)$_3$(Al)$_{4.5}$	0.6	3.7	5.7							1.33	1.69					6.2
2c(T^n)$_3$(T^m)$_{3.5}$(Al)$_5$		7.5	2.5							1.64	2.01					5.9
F−T/D/Al	T^1	T^2	T^3	D^0		D^1		D^2	T/D	T^2	T^3	D^1		D^2		
2a(T^n)$_3$(D^i)$_1$(Al)$_{2.5}$	1.0	4.4	4.6	0.2		0.4		2.6	3:1.0	0.90	1.28	0.83		0.97		5.5
2b(T^n)$_3$(D^i)$_{0.8}$(Al)$_{2.8}$	0.7	5.1	4.2			0.5		2.5	3:0.9	1.08	1.34	0.64		1.07		5.0
2c(T^n)$_3$(D^i)$_{0.8}$(Al)$_{5.3}$	0.6	4.8	4.6			1.1		1.4	3:0.8	2.19	2.22	1.01		1.54		5.6

[a] Calculated from eq 1 (see Experimental Section). [b] Determined by contact time variation. [c] Determined via ^{29}Si with experiment according to Schaefer.[33]

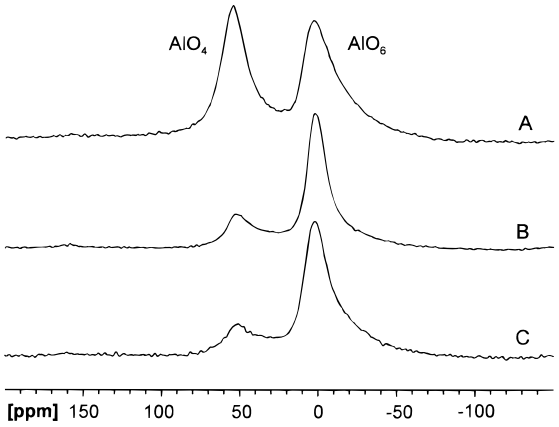

Figure 3. ^{27}Al MAS NMR spectra of the materials **2a(T^n)$_3$(Q^k)$_4$(Al)$_4$** (A), **2a(T^n)$_3$(T^m)$_{2.7}$(Al)$_{4.2}$** (B), and **2a(T^n)$_3$(D^i)$_1$(Al)$_{2.5}$** (C).

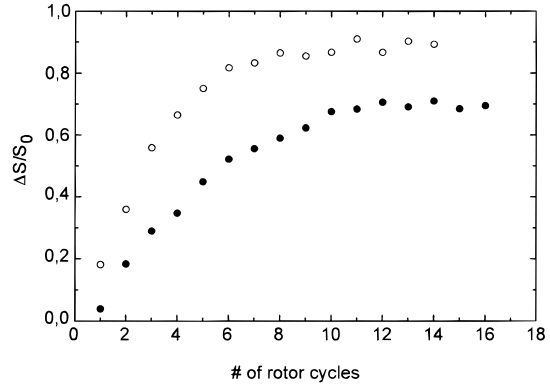

Figure 4. ^{27}Al{^{1}H}-REDOR signals, $\Delta S/S_0$, vs the number of rotor cycles of copolymer **2a(T^n)$_3$(Q^k)$_4$(Al)$_4$**. The MAS frequency is 10 kHz. Filled and open circles mark the AlO_4 (●) and AlO_6 (○) sites, respectively.

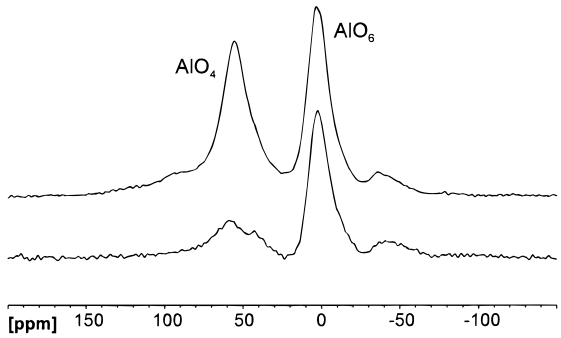

Figure 5. ^{1}H−^{27}Al CP/MAS (bottom) and ^{27}Al (SPE) MAS (top) NMR spectrum of copolymer **2a(T^n)$_3$(Q^k)$_4$(Al)$_4$**. The MAS frequency was 3 kHz.

The REDOR experiment serves to reintroduce the dipole−dipole interaction, which is canceled out by MAS. The dipole−dipole coupling depends on the distance between the nuclei and on the number of nuclei within certain distances. The REDOR experiment is a rotor-synchronized solid-state NMR double-resonance technique. During an echo sequence, which is applied on the nucleus under observation (e.g. ^{27}Al), π-pulses are irradiated on a second nucleus (e.g. ^{1}H). The time between π-pulses is synchronized with the rotor position. The difference of the intensities (ΔS) between the REDOR experiment (S_f) and a normal spin−echo experiment (S_0) depends on the duration of the echo period and the strength of the heteronuclear dipolar coupling. This allows one either to extract detailed structural information or at least to map out the environment of a nucleus.

The experimentally obtained ^{27}Al{^{1}H} REDOR curves of the copolymer **2a(T^n)$_3$(Q^k)$_4$(Al)$_4$** in which the REDOR fraction $\Delta S/S_0$ is plotted versus the number of rotor cycles are displayed in Figure 4. The shape of the REDOR curves is determined by the ^{27}Al−^{1}H dipolar interaction; for example, the steeper the slope of the REDOR curve, the stronger the dipolar interaction. Hence the dipolar interaction between the tetrahedrally coordinated AlO_4 sites and the protons is smaller than in the case of the octahedrally coordinated AlO_6 sites. In addition the final REDOR fraction of the AlO_6 groups approaches almost unity, indicating that all octahedrally coordinated aluminum atoms have protons in their proximity. The largest REDOR amplitude of the AlO_4 sites is only 0.7.

The results of the REDOR investigations are confirmed by the ^{1}H−^{27}Al CP/MAS spectrum of compound **2a(T^n)$_3$(Q^k)$_4$(Al)$_4$** (Figure 5). The signal of the 6-fold-coordinated AlO_6 sites is much larger in the CP/MAS NMR spectrum than that of the 4-fold-coordinated AlO_4 groups, whereas the resonances in the simple MAS NMR experiment are almost equal in intensity. From these results it is concluded that the AlO_6 groups contain numerous protons either as hydroxyl or as OH_2 ligands in their coordination sphere, whereas the AlO_4 sites are embedded in the matrixes in proton-poor areas, for example, as $Al(OSi)_4$ units. In other words, high

(26) Herzog, K.; Thomas, B.; Sprenger, D.; Jäger, C. *J. Non-Cryst. Solids* **1995**, *190*, 296.
(27) Morris, H. D.; Ellis, P. D. *J. Am. Chem. Soc.* **1989**, *111*, 6045.

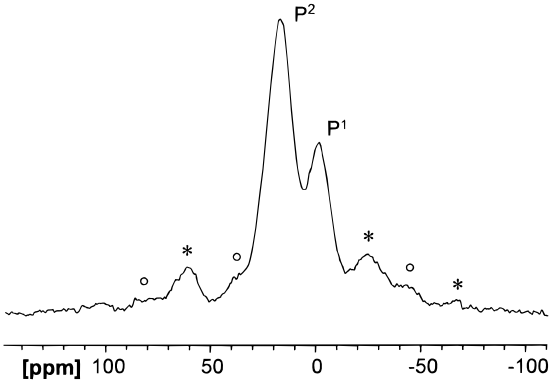

Figure 6. ^{31}P CP/MAS NMR spectrum of the poly(alumosiloxane)-bound ruthenium complex **2c(T^n)$_3$(Q^k)$_6$(Al)$_6$**. Open circles (○) and asteriks (*) denote spinning sidebands.

degrees of cross-linkage of the matrixes can only be obtained by high amounts of 4-fold-coordinated AlO_4 groups.

^{31}P, ^{13}C CP/MAS NMR and IR Spectroscopic Characterization of the Polymers. The ^{31}P CP/MAS NMR spectra of the immobilized ruthenium(II) complexes **2(a,b,c)(T^n)$_3$(Q^k, T^m, D^i)$_y$(Al)$_z$** show two isotropic signals caused by the different environments of the phosphorus nuclei P^1 and P^2 (Scheme 2 and Figure 6). Their chemical shifts are in agreement with their monomeric congeners (see Experimental Section).[19] The occurrence of only one absorption band in the carbonyl region of the IR spectra also confirms that the structure of the complex *cis*-H(Cl)Ru(CO)(P∼O)$_3$ is preserved during the sol−gel process.

The resonances in the ^{13}C CP/MAS NMR spectra of the polymers consist mainly of four groups of peaks belonging to the following species: the phenyl groups in the aromatic region at about 130 ppm, the carbon atoms of the ligands adjacent to the ether oxygen atoms [OCH_3 (58.0−58.8 ppm) and CH_2O (68.2−70.1 ppm)], a complex pattern of methylene groups in the region between 32 and 10 ppm, and in case of the F−T/T/Al and F−T/D/Al blends one signal of the $SiCH_3$ groups between −1 and −3 ppm. These chemical shifts clearly indicate the integrity of the phosphine ligands, in particular the existence of intact carbon−phosphorus and carbon−silicon bonds.[28]

Mobility Studies of the Immobilized Complexes by 2D WISE NMR Spectroscopy. Interphases are designed to be able to imitate homogeneous reaction types. Therefore a detailed knowledge of the dynamic behavior of the stationary phases is necessary to optimize the reactivity of the catalytic centers. Higher mobilities of the immobilized catalysts should enhance the accessibility and the uniformity of the reactive centers and thus their activities as well as their selectivities. The line widths of the protons in the two-dimensional WISE spectra are sensitive toward motions.

The pulse sequence of the WISE experiment consists of an ^{1}H $\pi/2$ pulse followed by an incremented proton evolution time (t_1), after which the proton magnetization is transferred to ^{13}C via Hartmann−Hahn cross polarization, that is, $\pi/2(^1H)-t_1-CP-$acquisition.[17] Slices at individual ^{13}C resonances in a 2D data set reveal the

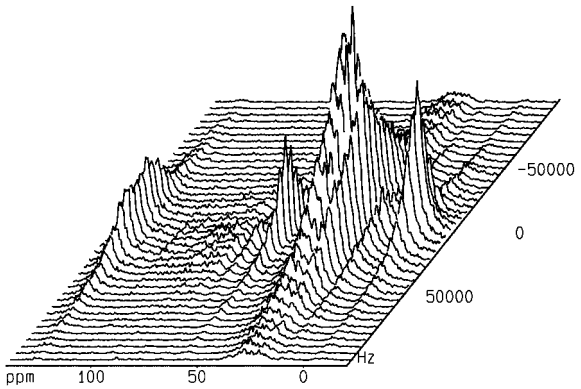

Figure 7. WISE spectrum of the polymer bound complex **2c-(T^n)$_3$(T^m)$_{3.5}$(Al)$_5$**. The F2 dimension (^{13}C) contains the structural information, whereas the line widths in the F1 dimension (protons) reveal the mobility of the individual parts of the polymer.

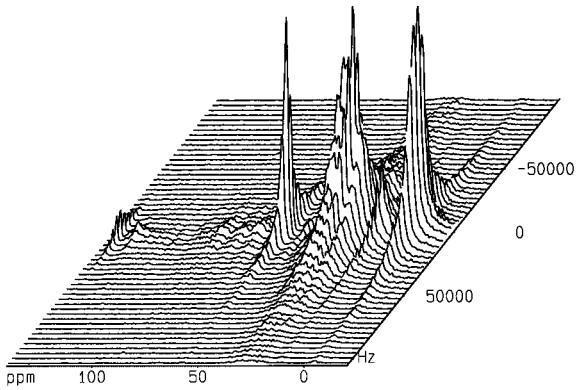

Figure 8. WISE spectrum of the polymer-bound complex **2c-(T^n)$_3$(T^m)$_{3.5}$(Al)$_5$** suspended in toluene-d_8. Because of the swelling of the material, the line widths in the F1 dimension are reduced by the factor 2.

^{1}H line widths of the various structural moieties within a sample. The line widths in the F1 (proton) dimension are determined by ^{1}H−^{1}H dipolar interactions, which are reduced by molecular motion and magic-angle spinning.

In Figure 7 the WISE spectrum of the polymer **2c-(T^n)$_3$(T^m)$_{3.5}$(Al)$_5$** is depicted. The line widths in the F1 dimension of the methylene groups (18 and 25−31 ppm) and of the aromatic region are about 50 kHz. Because of their fast rotation, the methyl groups ($SiCH_3$ at −3 ppm and OCH_3 at 58 ppm) show smaller line widths. This is comparable with earlier investigations on pure polysiloxane matrixes which reveal that the high degrees of cross-linkage in these systems lead to uniformly rigid matrixes.[11] For the catalytic application of these materials which act as stationary phases in interphases it is also of interest to study the dynamic behavior of the polymer under the influence of an adequate mobile phase. The corresponding WISE spectrum of compound **2c(T^n)$_3$(T^m)$_{3.5}$(Al)$_5$** suspended in toluene-d_8 is displayed in Figure 8. Reasonable line narrowing of resonances in the F1 dimension (25 kHz for the methylene groups and 10 kHz for the methyl groups) indicates enhanced flexibilities of all structural moieties under the influence of the solvent.

Catalytic Activity of the Materials. α,β-Unsaturated aldehydes are easily accessible through aldol condensation of aldehydes. The selective hydrogenation

(28) Corriu, R. J. P.; Moreau, J. J. E.; Thepot, P.; Wong Chi Man, M. *J. Mater. Chem.* **1994**, *4*, 987.

Table 4. Hydrogenation of 2-Butenal[a]

run	catalyst	spacer	surface area [m²/g]	conversion [%]	selectivity [%]		
					n-butanal	2-butenol	*n*-butanol
	F−T/Q/Al						
1	**2a**$(T^n)_3(Q^k)_4(Al)_4$[b]	*n*-propyl	60	35	28	60	12
2	**2b**$(T^n)_3(Q^k)_5(Al)_{4.3}$	*n*-hexyl	45	37	23	63	14
3	**2c**$(T^n)_3(Q^k)_6(Al)_6$	*n*-octyl	50	38	23	60	17
	F−T/T/Al						
4	**2a**$(T^n)_3(T^m)_{2.7}(Al)_{4.2}$	*n*-propyl	120	52	17	62	21
5	**2b**$(T^n)_3(T^m)_3(Al)_{4.5}$	*n*-hexyl	60	48	18	63	19
6	**2c**$(T^n)_3(T^m)_{3.5}(Al)_5$	*n*-octyl	70	47	18	59	22
	F−T/D/Al						
7	**2a**$(T^n)_3(D^i)_1(Al)_{2.5}$[c]	*n*-propyl	75	71	11	65	24
8	**2b**$(T^n)_3(D^i)_{0.8}(Al)_{2.8}$	*n*-hexyl	50	69	12	64	22
9	**2c**$(T^n)_3(D^i)_{0.8}(Al)_{5.3}$	*n*-octyl	75	60	15	64	21

[a] H_2 pressure = 50 bar, Ru/*n*-butenal = 1:1000, temperature = 120 °C, reaction time = 1 h. [b] Second run with 33% conversion and third run with 34% conversion. [c] Second run with 65% conversion and third run with 64% conversion.

of the C═O double bond to the corresponding alcohol is thus a way to obtain particular substituted alcohols. Various ruthenium complexes have been proved to show high activities toward the selective hydrogenation of C═O versus C═C double bonds in model reactions with homogeneous as well as heterogeneous catalysts.[7,14,29−32]

In this work we employed *n*-butenal as a model substrate. The expected hydrogenation products are *n*-butanal, 2-butenol, and *n*-butanol. In the course of the catalytic reaction an increasing formation of side products (10%) is caused by condensation reactions of the crotylaldehyde.

The results of the hydrogenation experiments and the BET surface areas of the catalysts are displayed in Table 4. The F−T/Q/Al copolymers show conversions in the range 35−38% (run 1−3). The selectivities in the formation of the unsaturated alcohol compared to the formation of the saturated aldehyde are about 2.5:1 for these catalysts. Variation of the matrixes leads to higher conversions, for example, ca. 50% for the F−T/T/Al-anchored catalysts (run 4−6) and ca. 70% for the F−T/D/Al copolymers. Thereby an increasing chemoselectivity toward the hydrogenation of the C═O double bond is observed (run 7: 2-butenol/*n*-butanal = 5:1). An enhanced formation of the dihydrogenation product *n*-butanol is observed for the faster catalysts (run 7−9).

From measurements of the BET surface areas it is assumed that diffusion of the substrate into the matrix is not the overall rate-determining step which causes the different activities of the catalysts. The dynamic solid-state NMR investigations suggest that the mobility of the reactive centers is determined by the lengths of the spacers and not by the type of the co-condensation agent, indicating that different swelling behavior of the different copolymers leads to the observed catalytic properties. The high cross-linked F−T/Q/Al copolymers are obviously less favored to swell under the influence of the reaction mixture than the less cross-linked F−T/T/Al or F−T/D/Al matrixes.

The catalysts can be fully recycled from the reaction mixtures by simple centrifugation after a catalytic run. Thereby the supernatant reaction mixture does not show any catalytic activity. After washing with acetone and *n*-hexane and drying under vacuo the catalysts can be reused with constant catalytic activity.

Conclusion

In this study we have demonstrated that the sol−gel method offers a way to immobilize catalytic-active ruthenium complexes on poly(alumosiloxane) supports. To transfer the large variety of "pure" polysiloxanes, three different silyl-containing co-condensation agents (**Q^0**, **T^0**, **D^0**) have been employed. 2D WISE NMR experiments on dry and suspended (toluene-d_8) materials illustrate the increase of mobility of all structural moieties, which is important in forming an interphase. Thus the materials show remarkable activities and selectivities in the hydrogenation of *n*-butenal. The differences in the catalytic activity of the materials can be traced back to the different swelling behavior of the matrixes.

Experimental Section

Characterization. Elemental analyses were carried out on a Carlo Erba analyzer, model 1106. IR data were obtained on a Bruker IFS 48 FT-IR spectrometer. The scanning electron micrograph and the EDX data were measured with a Philips scanning electron microscope XL 30-FEG equipped with an EDAX DX-4 spectrometer system with ultrathin window ($Z > 5$ detectable). Beam voltages between 10 and 30 kV were used. External standards were used for the quantititave determination of the elements. Thereby limits of error for the individual elements are smaller than ±10% except for carbon and oxygen. The sample was sputtered with platinum to form layers of 15−20-nm thickness for recording the micrograph. The surface areas were determined by nitrogen sorption and calculated with the BET equation on a Micromeritics Gemini 2375.

The MAS solid-state NMR spectra were recorded on Bruker multinuclear spectrometers with wide bore magnets (MSL 200, 4.7 T, ^{29}Si; ASX 300, 7.05 T, ^{13}C, ^{27}Al, ^{31}P) using samples of 100−400 mg in double-bearing rotors of ZrO_2. Magic-angle spinning was performed at 10-12 kHz (^{13}C, ^{27}Al), 3.3 kHz (^{29}Si), and 5 kHz (^{31}P) at room temperature. The spectra were taken using either cross polarization (^{29}Si, ^{31}P, ^{27}Al, ^{13}C) or single-pulse excitation (^{27}Al, ^{29}Si) with high-power decoupling in all cases. All measurements were carried out under the exclusion of molecular oxygen. Frequencies, standards and parameters: ^{29}Si, 39.75 MHz (Q_8M_8), contact time 3−5 ms, recycle delay 2 s (CP MAS) and 100 s (MAS), T_{SiH} by variations of the contact time (15−20 suitable experiments), $T_{1\rho H}$ by a spin lock-τ-CP experiment as described by Schaefer and

(29) Cornils, B.; Feichtinger, H. *Chem. Z.* **1977**, *101*, 107.
(30) Broucková, Z.; Czaková, M.; Capka, M. *J. Mol. Catal.* **1985**, *30*, 241.
(31) Strohmeier, W.; Holke, K. *J. Organomet. Chem.* **1980**, *193*, C63.
(32) Fache, E.; Mercier, C.; Pagnier, N.; Despeyroux, B.; Panster, P. *J. Mol. Catal.* **1993**, *79*, 117.

Stejskal.[33] $T_{1\rho H}$ relaxation data were obtained using Bruker software SIMFIT. Peak deconvolution of the spectra was performed with the Bruker-Spectrospin software XNMR using Voigtian line shapes. The relative amounts I_0 of each of the D^i, $T^{n,m}$, and Q^k species were calculated by inserting their peak areas of the deconvoluted spectra $I(T_c)$, the individual T_{SiH} data, and the common $T_{1\rho H}$ value into the following equation:[34]

$$I_{(Tc)} = \frac{I_0}{(1 - T_{SiH}/T_{1\rho H})}(e^{-T_c/T_{1\rho H}} - e^{-T_c/T_{SiH}})$$

Thereby the boundary condition $T_{SiH} \ll T_{1\rho H}$ was fulfilled for all samples: ^{13}C, 75.470 MHz [TMS, carbonyl resonance of glycine ($\delta = 176.03$) as the second standard], contact time 2 ms, recycle delay 4 s. The WISE NMR spectra were recorded under MAS conditions (4 kHz). Between 40 and 64 t_1 increments with a dwell time of 3−5 μs were used for each spectrum. Cross polarization was applied with contact times between 200 and 300 μs: ^{31}P, 121.49 MHz [85% H_3PO_4, $NH_4H_2PO_4$ ($\delta = 0.8$) as the second standard], contact time 1 ms, recycle delay 2 s; ^{27}Al, 78.20 MHz [0.1 M aqueous solution of $Al(NO_3)_3$], pulse length 0.6 μs ($\leq\pi/12$ pulse), recycle delay 500 ms. ^{27}Al chemical shifts are (as the data published in the literature) not corrected for second-order quadrupolar shifts. The REDOR experiments have been performed at MAS frequencies of 12 kHz. The 180° proton pulse length was 10 μs, and the 90° pulses for ^{27}Al were 2.2 μs. The $^{27}Al-^{1}H$ CP/MAS NMR spectra were recorded with a contact time of 300 μs, an ^{1}H $\pi/2$ pulse of 5 μs, a recycle delay of 1 s, and spinning rates of 3 kHz. The Hartmann−Hahn condition of $3\gamma_{Al}B_{Al} = \gamma_H B_H$ was adjusted by changing the power in the Al channel to get a maximum signal.[27] For a more detailed description of other NMR parameters see ref 6.

Catalysis. The hydrogenation experiments were carried out in 100-mL autoclaves under exclusion of oxygen [argon, 150 μmol catalyst with respect to ruthenium, 150 mmol of *n*-butenal]. The analyses were performed quantitatively on a GC 6000 Vega Series 2 (Carlo Erba Instruments) with a FID and a capillary column SP 1000 [60 m; carrier gas, He (50 kPa); integrator, 3393 A (Hewlett-Packard)].

Synthesis. All manipulations were performed under argon by employing the usual Schlenk techniques. Methanol was dried with magnesium and distilled from $Mg(OMe)_2$; ethanol was distilled from NaOEt. Acetone was distilled from P_4O_{10}. *n*-Hexane and toluene were distilled from sodium benzophenone ketyl. H_2O, $Si(OEt)_4$ (**Q⁰**) (Aldrich), $MeSi(OMe)_3$ (**T⁰**) (Aldrich), and $Me_2Si(OEt)_2$ (**D⁰**) (Aldrich) were distilled under inert gas prior to use. All solvents were stored under argon. The monomeric complexes **2(a,b,c)(T⁰)₃** were synthesized as previously described.[10]

Sol−Gel Processing. Finely ground $Al(OiPr)_3$ was dispersed in 10 mL of methanol and 3 mL of water. The resulting sol was added to a mixture of the corresponding monomeric complex **2(a,b,c)(T⁰)₃**, the co-condensate $Si(OEt)_4$ (**Q⁰**), $MeSi(OMe)_3$ (**T⁰**), or $Me_2Si(OEt)_2$ (**D⁰**), water, and $(n\text{-}Bu)_2Sn(OAc)_2$. This mixture was stirred in a sealed Schlenk tube for 2 h at room temperature. After adding specific amounts of aqueous 2 M NaOH the mixture was stirred for 16 h. Then methanol was removed in vacuo. Subsequently a saturated solution of NH_4HCO_3 (10 mL) was added dropwise under stirring. After 2 h the resulting precipitates were isolated by centrifugation and washed with an 1 M aqueous solution of NH_4HCO_3 and water (5 times each with 10 mL), then dried with acetone (5 times each with 10 mL), and stirred in *n*-hexane (twice with 50 mL, 4 h). Final aging of the materials was carried out by drying at 60 °C under vacuum for 8 h (densities 0.2−0.3 g/mL).

Carbonylchlorohydridotris[(2-methoxyethyl)phenyl(poly(alumosiloxanyl)propyl)phosphine-*P,P',P''*]ruthenium(II)(Q)₄(Al)₄ [2a(T^n)₃(Q^k)₄(Al)₄]. A mixture of $HRuCl(CO)(P{\sim}O)_3$ [**2a(T⁰)₃**] (459 mg, 0.40 mmol), 6 equiv of $Si(OEt)_4$ (**Q⁰**) (524 mg, 2.38 mmol), 6 equiv of $Al(OiPr)_3$ (488 mg, 2.38 mmol), and $(n\text{-}Bu)_2Sn(OAc)_2$ (10 mg, 0.03 mmol) was sol−gel processed to give a gray gel (600 mg, 94%): ^{13}C CP/MAS NMR δ 18.1 (CH_2Si), 27.3 ($CH_2CH_2CH_2Si$, $PCH_2CH_2OCH_3$), 49.8 ($SiOCH_3$), 58.1 (CH_2OCH_3), 68.1 ($PCH_2CH_2OCH_3$), 128.7 (C_{arom}); ^{27}Al MAS (SPE) NMR δ 3 (AlO_6), 55 (AlO_4); ^{29}Si CP/MAS NMR (silicon substructure) −47 (T^1), −55/−59 (T^2), −65 (T^3), −82 (Q^0), −86 (Q^1), −91 (Q^2), −98 (Q^3), −109 (Q^4); ^{31}P CP/MAS NMR δ 17.5 (P^2, $\nu_{1/2} = 2890$ Hz), −1.0 (P^1); IR (KBr, cm^{-1}) 1923 [ν(CO)]. Anal. Calcd for $C_{37}H_{77}Al_4ClO_{32.5}P_3RuSi_7$ (corrected stoichiometry):[35] C, 27.91; H, 4.87; Cl, 2.23; Ru, 6.35. Found: C, 28.95; H, 4.88; Cl, 1.97; Ru, 5.90.

Carbonylchlorohydridotris[(2-methoxyethyl)phenyl(poly(alumosiloxanyl)hexyl)phosphine-*P,P',P''*]ruthenium(II)(Q)₅(Al)$_{4.3}$ [2b(T^n)₃(Q^k)₅(Al)$_{4.3}$]. A mixture of $HRuCl(CO)(P{\sim}O)_3$ [**2b(T⁰)₃**] (499 mg, 0.40 mmol), 6 equiv of $Si(OEt)_4$ (**Q⁰**) (524 mg, 2.38 mmol), 6 equiv of $Al(OiPr)_3$ (488 mg, 2.38 mmol), and $(n\text{-}Bu)_2Sn(OAc)_2$ (13 mg, 0.04 mmol) was sol−gel processed to give a gray gel (454 mg, 61%): ^{13}C CP/MAS NMR δ 13.7 (CH_2Si), 26.7 [CH_2CH_2Si, $PCH_2(CH_2)_5$], 30.1 [$PCH_2(CH_2)_3$, $PCH_2CH_2OCH_3$], 58.0 (CH_2OCH_3), 68.4 ($PCH_2CH_2OCH_3$), 128.9 (C_{arom}); ^{27}Al MAS (SPE) NMR δ 3 (AlO_6), 55 (AlO_4); ^{29}Si CP/MAS NMR (silicon substructure) −48 (T^1), −55/−58 (T^2), −65 (T^3), −82 (Q^0), −87 (Q^1), −93 (Q^2), −100 (Q^3), −110 (Q^4); ^{31}P CP/MAS NMR δ 18.5 (P^2, $\nu_{1/2} = 2170$ Hz), 0.4 (P^1); IR (KBr, cm^{-1}) 1917 [ν(CO)]. Anal. Calcd for $C_{49}H_{98.6}Al_{4.3}ClO_{32.05}P_3RuSi_8$ (corrected stoichiometry):[35] C, 31.76; H, 5.36; Cl, 1.91; Ru, 5.46. Found: C, 30.62; H, 5.09; Cl, 1.80; Ru, 5.01.

Carbonylchlorohydridotris[(2-methoxyethyl)phenyl(poly(alumosiloxanyl)octyl)phosphine-*P,P',P''*]ruthenium(II)(Q)₆(Al)₆ [2c(T^n)₃(Q^k)₆(Al)₆]. A mixture of $HRuCl(CO)(P{\sim}O)_3$ [**2c(T⁰)₃**] (855 mg, 0.63 mmol), 6 equiv of $Si(OEt)_4$ (**Q⁰**) (781 mg, 3.75 mmol), 6 equiv of $Al(OiPr)_3$ (768 mg, 3.75 mmol), and $(n\text{-}Bu)_2Sn(OAc)_2$ (13 mg, 0.04 mmol) was sol−gel processed to give a gray gel (825 mg, 63%): ^{13}C CP/MAS NMR δ 13.9 (CH_2Si), 28.0 [CH_2CH_2Si, $PCH_2(CH_2)_7$], 30.1 [$PCH_2(CH_2)_5$, $PCH_2CH_2OCH_3$], 49.2 ($SiOCH_3$), 58.0 (CH_2OCH_3), 68.2 ($PCH_2CH_2OCH_3$), 128.5 (C_{arom}); ^{27}Al MAS (SPE) NMR δ 4 (AlO_6), 55 (AlO_4); ^{29}Si CP/MAS NMR (silicon substructure) −50 (T^1), −56/−59 (T^2), −65 (T^3), −81 (Q^0), −86 (Q^1), −92 (Q^2), −100 (Q^3), −110 (Q^4); ^{31}P CP/MAS NMR δ 18.4 (P^2, $\nu_{1/2} = 1870$ Hz), −1.0 (P^1); IR (KBr, cm^{-1}) 1915 [ν(CO)]. Anal. Calcd for $C_{52}H_{115}Al_6ClO_{44.5}P_3RuSi_9$ (corrected stoichiometry):[35] C, 29.79; H, 5.53; Cl, 1.69; Ru, 4.48. Found: C, 28.95; H, 5.34; Cl, 1.43; Ru, 4.03.

Carbonylchlorohydridotris[(2-methoxyethyl)phenyl(poly(alumosiloxanyl)propyl)phosphine-*P,P',P''*]ruthenium(II)(T)$_{2.7}$(Al)$_{4.2}$ [2a(T^n)₃(T^m)$_{2.7}$(Al)$_{4.2}$]. A mixture of $HRuCl(CO)(P{\sim}O)_3$ [**2a(T⁰)₃**] (459 mg, 0.40 mmol), 6 equiv of $MeSi(OMe)_3$ (**T⁰**) (325 mg, 2.38 mmol), 6 equiv of $Al(OiPr)_3$ (488 mg, 2.38 mmol), and $(n\text{-}Bu)_2Sn(OAc)_2$ (10 mg, 0.03 mmol) was sol−gel processed to give a gray gel (523 mg, 86%): ^{13}C CP/MAS NMR δ −2.9 ($SiCH_3$), 18.0 (CH_2Si), 26.5 ($CH_2CH_2CH_2Si$, $PCH_2CH_2OCH_3$), 50.0 ($SiOCH_3$), 57.5 (CH_2OCH_3), 67.6 ($PCH_2CH_2OCH_3$), 128.4 (C_{arom}); ^{27}Al MAS (SPE) NMR δ 2 (AlO_6), 53 (AlO_4); ^{29}Si CP/MAS NMR (silicon substructure) −47 (T^1), −54/−57 (T^2), −64 (T^3); ^{31}P CP/MAS NMR δ 16.5 (P^2, $\nu_{1/2} = 2530$ Hz), −0.8 (P^1); IR (KBr, cm^{-1}) 1922 [ν(CO)]. Anal. Calcd for $C_{39.7}H_{82.9}Al_{4.2}ClO_{28.75}P_3RuSi_{5.7}$ (corrected stoichiometry):[35] C, 31.30; H, 5.48; Cl, 2.33; Ru, 6.64. Found: C, 31.47; H, 5.24; Cl, 2.03; Ru, 6.39.

Carbonylchlorohydridotris[(2−methoxyethyl)phenyl(poly(alumosiloxanyl)hexyl)phosphine-*P,P',P''*]ruthenium(II)(T)$_3$(Al)$_{4.5}$ [2b(T^n)₃(T^m)₃(Al)$_{4.5}$]. A mixture of $HRuCl(CO)(P{\sim}O)_3$ [**2b(T⁰)₃**] (499 mg, 0.40 mmol), 6 equiv of $MeSi(OMe)_3$ (**T⁰**) (325 mg, 2.38 mmol), 6 equiv of $Al(OiPr)_3$ (488

(33) Schaefer, J.; Stejskal, E. O.; Buchdahl, R. *Macromolecules* **1977**, *10*, 384.

(34) Harris, R. K. *Analyst* **1985**, *110*, 649.

(35) The broken numbers in the chemical formulas are due to the composition of the materials under consideration of the EDX results. The corrected stoichiometry was obtained by adding an additional number of H_2O molecules to the polymer unit. It was one molecule H_2O per silicon or aluminum atom. This approximation is reasonable for uncondensed Si−OH or Al−OH groups and physisorbed water.

mg, 2.38 mmol), and $(n\text{-Bu})_2Sn(OAc)_2$ (10 mg, 0.03 mmol) was sol−gel processed to give a gray gel (553 mg, 80%): ^{13}C CP/MAS NMR δ 1.3 ($SiCH_3$), 13.8 (CH_2Si), 26.4 [CH_2CH_2Si, $PCH_2(CH_2)_5$], 30.0 [$PCH_2(CH_2)_3$, $PCH_2CH_2OCH_3$], 57.8 (CH_2OCH_3), 68.1 ($PCH_2CH_2OCH_3$), 128.4 (C_{arom}); ^{27}Al MAS (SPE) NMR δ 2 (AlO_6), 53 (AlO_4); ^{29}Si CP/MAS NMR (silicon substructure) −48 (T^1), −56/−59 (T^2), −65 (T^3); ^{31}P CP/MAS NMR δ 17.5 (P^2, $\nu_{1/2}$ = 2030 Hz), −1.1 (P^1); IR (KBr, cm^{-1}) 1918 [ν(CO)]. Anal. Calcd for $C_{52}H_{103}Al_{4.5}ClO_{30.25}P_3RuSi_6$ (corrected stoichiometry):[35] C, 36.06; H, 6.00; Cl, 2.05; Ru, 5.84. Found: C, 33.51; H, 5.98; Cl, 1.77; Ru, 5.32.

Carbonylchlorohydridotris[(2−methoxyethyl)phenyl-(poly(alumosiloxanyl)octyl)phosphine-*P,P',P''*]ruthenium-(II)$(T)_{3.5}(Al)_5$ [2c$(T^n)_3(T^m)_{3.5}(Al)_5$]. A mixture of $HRuCl(CO)(P{\sim}O)_3$ [**2c$(T^0)_3$**] (855 mg, 0.63 mmol), 6 equiv of $MeSi(OMe)_3$ (**T^0**) (511 mg, 3.75 mmol), 6 equiv of $Al(OiPr)_3$ (768 mg, 3.75 mmol), and $(n\text{-Bu})_2Sn(OAc)_2$ (13 mg, 0.04 mmol) was sol−gel processed to give a gray gel (893 mg, 76%): ^{13}C CP/MAS NMR δ −3.0 ($SiCH_3$), 13.8 (CH_2Si), 26.9 [CH_2CH_2Si, $PCH_2(CH_2)_7$], 30.5 [$PCH_2(CH_2)_5$, $PCH_2CH_2OCH_3$], 58.1 (CH_2OCH_3), 68.3 ($PCH_2CH_2OCH_3$), 128.4 (C_{arom}); ^{27}Al MAS (SPE) NMR δ 3 (AlO_6), 53 (AlO_4); ^{29}Si CP/MAS NMR (silicon substructure) −58 (T^2), −66 (T^3); ^{31}P CP/MAS NMR δ 17.0 (P^2, $\nu_{1/2}$ = 1870 Hz), −0.5 (P^1); IR (KBr, cm^{-1}) 1916 cm^{-1} [ν(CO)]. Anal. Calcd for $C_{55.5}H_{118.5}Al_5ClO_{32.75}P_3RuSi_{6.5}$ (corrected stoichiometry):[35] C, 35.90; H, 6.43; Cl, 1.91; Ru, 5.44. Found: C, 34.35; H, 6.24; Cl, 1.47; Ru, 4.90.

Carbonylchlorohydridotris[(2-methoxyethyl)phenyl-(poly(alumosiloxanyl)propyl)phosphine-*P,P',P''*]-ruthenium(II)$(D)_1(Al)_{2.5}$ [2a$(T^n)_3(D^i)_1(Al)_{2.5}$]. A mixture of $HRuCl(CO)(P{\sim}O)_3$ [**2a$(T^0)_3$**] (459 mg, 0.40 mmol), 6 equiv of $Me_2Si(OEt)_2$ (**D^0**) (354 mg, 2.38 mmol), 6 equiv of $Al(OiPr)_3$ (488 mg, 2.38 mmol), and $(n\text{-Bu})_2Sn(OAc)_2$ (10 mg, 0.03 mmol) was sol−gel processed to give a gray gel (446 mg, 88%): ^{13}C CP/MAS NMR δ −1.3 ($SiCH_3$), 18.1 (CH_2Si), 26.7 (CH_2CH_2-CH_2Si, $PCH_2CH_2OCH_3$), 49.6 ($SiOCH_3$), 57.9 (CH_2OCH_3), 68.2 ($PCH_2CH_2OCH_3$), 128.7 (C_{arom}); ^{27}Al MAS (SPE) NMR δ 2 (AlO_6), 51 (AlO_4); ^{29}Si CP/MAS NMR (silicon substructure) −9 (D^0), −12/−15 (D^1), −21(D^2), −49 (T^1), −56 (T^2), −65 (T^3); ^{31}P CP/MAS NMR δ 18.6 (P^2, $\nu_{1/2}$ = 2440 Hz), 0.2 (P^1); IR (KBr, cm^{-1}) 1919 cm^{-1} [ν(CO)]. Anal. Calcd for $C_{39}H_{74}Al_{2.5}ClO_{19.75}P_3$-$RuSi_4$ (corrected stoichiometry):[35] C, 36.93; H, 5.88; Cl, 2.80; Ru, 7.97. Found: C, 36.58; H, 5.60; Cl, 2.68; Ru, 6.93.

Carbonylchlorohydridotris[(2-methoxyethyl)phenyl-(poly(alumosiloxanyl)hexyl)phosphine-*P,P',P''*]-ruthenium(II)$(D)_{0.8}(Al)_{2.8}$ [2b$(T^n)_3(D^i)_{0.8}(Al)_{2.8}$]. A mixture of $HRuCl(CO)(P{\sim}O)_3$ [**2b$(T^0)_3$**] (499 mg, 0.40 mmol), 6 equiv of $Me_2Si(OEt)_2$ (**D^0**) (354 mg, 2.38 mmol), 6 equiv of $Al(OiPr)_3$ (488 mg, 2.38 mmol), and $(n\text{-Bu})_2Sn(OAc)_2$ (10 mg, 0.03 mmol) was sol−gel processed to give a gray gel (477 mg, 83%): ^{13}C CP/MAS NMR δ 1.2 ($SiCH_3$), 13.9 (CH_2Si), 26.9 [CH_2CH_2Si, $PCH_2(CH_2)_5$], 30.5 [$PCH_2(CH_2)_3$, $PCH_2CH_2OCH_3$], 58.0 (CH_2OCH_3), 68.1 ($PCH_2CH_2OCH_3$), 128.7 (C_{arom}); ^{27}Al MAS (SPE) NMR δ 3 (AlO_6), 51 (AlO_4); ^{29}Si CP/MAS NMR (silicon substructure) −13 (D^1), −22 (D^2), −48 (T^1), −56/−59 (T^2), −66 (T^3); ^{31}P CP/MAS NMR δ 18.0 (P^2, $\nu_{1/2}$ = 2010 Hz), −0.5 (P^1); IR (KBr, cm^{-1}) 1915 cm^{-1} [ν(CO)]. Anal. Calcd for $C_{50.6}H_{91}$-$Al_{2.8}ClO_{20.1}P_3RuSi_{3.8}$ (corrected stoichiometry):[35] C, 42.42; H, 6.40; Cl, 2.47; Ru, 7.06. Found: C, 39.55; H, 6.23; Cl, 1.99; Ru, 6.14.

Carbonylchlorohydridotris[(2-methoxyethyl)phenyl-(poly(alumosiloxanyl)octyl)phosphine-*P,P',P''*]ruthenium-(II)$(D)_{0.8}(Al)_{5.3}$ [2c$(T^n)_3(D^i)_{0.8}(Al)_{5.3}$]. A mixture of $HRuCl(CO)(P{\sim}O)_3$ [**2c$(T^0)_3$**] (855 mg, 0.63 mmol), 6 equiv of $Me_2Si(OEt)_2$ (**D^0**) (556 mg, 3.75 mmol), 6 equiv of $Al(OiPr)_3$ (768 mg, 3.75 mmol), and $(n\text{-Bu})_2Sn(OAc)_2$ (13 mg, 0.04 mmol) was sol−gel processed to give a gray gel (719 mg, 69%): ^{13}C CP/MAS NMR δ 1.3 ($SiCH_3$), 13.8 (CH_2Si), 26.8 [CH_2CH_2Si, $PCH_2(CH_2)_7$], 29.9 [$PCH_2(CH_2)_5$, $PCH_2CH_2OCH_3$], 57.9 (CH_2OCH_3), 67.8 ($PCH_2CH_2OCH_3$), 128.6 (C_{arom}); ^{27}Al MAS (SPE) NMR δ 3 (AlO_6), 51 (AlO_4); ^{29}Si CP/MAS NMR (silicon substructure) −9 (D^0), −14/−19 (D^1), −23 (D^2), −48 (T^1), −55/−58 (T^2), −65 (T^3); ^{31}P CP/MAS NMR δ 18.2 (P^2, $\nu_{1/2}$ = 1900 Hz), −0.3 (P^1); IR (KBr, cm^{-1}) 1915 cm^{-1} [ν(CO)]. Anal. Calcd for $C_{53.5}H_{109.6}Al_{5.3}ClO_{26.35}P_3RuSi_{3.8}$ (corrected stoichiometry):[35] C, 38.83; H, 6.68; Cl, 2.14; Ru, 6.11. Found: C, 35.51; H, 6.40; Cl, 1.78; Ru, 5.12.

Acknowledgment. The support of this research by the Deutsche Forschungsgemeinschaft (Forschergruppe, Grant No. Li 154/41-3, and Forschergruppe, Grant No. Go 301/23-1) Bonn/Bad Godesberg, and by the Fonds der Chemischen Industrie, Frankfurt/Main is gratefully acknowledged. We are thankful for helpful discussions with Dr. Christian Jäger, University of Jena. Furthermore we thank Prof. K. G. Nickel, Institut für Mineralogie, University of Tübingen, and Dipl.-Chem. W. Wielandt, Institut für Anorganische Chemie, University of Tübingen, for BET measurements. A.J. thanks the Fonds der Chemischen Industrie for a Doktorandenstipendium.

CM970342C